Finite Elements in Analysis and Design 45 (2009) 263 – 271

Contents lists available at ScienceDirect

Finite Elements in Analysis and Design

journal homepage: www.elsevier.com/locate/finel

A posteriori error analysis for a transient conjugate heat transfer problem

D. Estep[a,b,1], S. Tavener[a,2], T. Wildey[c,*,3]

[a] *Department of Mathematics, Colorado State University, Fort Collins, CO 80523, USA*
[b] *Department of Statistics, Colorado State University, Fort Collins, CO 80523, USA*
[c] *Institute for Computational Engineering and Sciences, The University of Texas, Austin, TX 78712, USA*

ARTICLE INFO

Article history:
Received 2 September 2008
Accepted 13 October 2008
Available online 24 December 2008

MSC:
65N15
65N30
65N50

Keywords:
A posteriori error analysis
Adaptive mesh refinement
Adjoint problem
Boundary flux method
Conjugate heat transfer
Finite element method
Generalized Green's function
Goal oriented error estimates
Operator decomposition
Residual
Transfer error

ABSTRACT

We consider the accuracy of an operator decomposition finite element method for a transient conjugate heat transfer problem consisting of two materials coupled through a common boundary. We derive accurate *a posteriori* error estimates that account for the transfer of error between components of the operator decomposition method as well as the errors in solving the iterative system. We address a loss of order of convergence that results from the decomposition, and show that the order of convergence is limited by the accuracy of the transferred gradient information. We extend a boundary flux recovery method to transient problems and use it to regain the expected order of accuracy in an efficient manner. In addition, we use the *a posteriori* error estimates to adaptively compute the recovered boundary flux only within the domain of dependence for a quantity of interest.

1. Introduction

In this paper, we consider the solution to a conjugate heat transfer problem by an operator decomposition approach. The goal is to compute a functional of the temperature of a body composed of two distinct components that share a common boundary or interface. The two components may have different conductivities and be subject to different heat sources and boundary conditions. The model consists a pair of parabolic differential equations in abutting regions that are coupled through boundary conditions posed at the common interface.

One approach to solve a multi-physics problem is to directly discretize the global system and to solve the resulting large set of equations. However, there are situations in which this approach is infeasible, e.g. because of the size of the full global system or because different numerical methods and codes are to be used for the component problems.

Alternately, we apply operator decomposition, which is a widely used technique for solving multi-physics, multi-scale problems. The general approach is to decompose the problem into components involving simpler physics over a relatively limited range of scales, and then to seek the solution to the entire system through an iterative procedure involving solutions to the individual components. This approach is appealing because there is generally a good understanding of how to solve a broad spectrum of single physics problems accurately and efficiently, and because it provides an alternative to accommodating multiple scales in one discretization by allowing different discretizations for different components. However, operator decomposition presents an entirely new set of accuracy and stability issues, some of which are obvious and some subtle, and all of which

* Corresponding author.
E-mail addresses: estep@math.colostate.edu (D. Estep), tavener@math.colostate.edu (S. Tavener), twildey@ices.utexas.edu (T. Wildey).

[1] The author's work is supported in part by the Department of Energy (DE-FG02-04ER25620, DE-FG02-05ER25699, and DE-FC02-07ER54909), Lawrence Livermore National Laboratory (B573139), the National Aeronautics and Space Administration (NNG04GH63G), the National Science Foundation (DMS-0107832, DMS-0715135, DGE-0221595003, MSPA-CSE-0434354, and ECCS-0700559), Idaho National Laboratory (00069249), and the Sandia Corporation (PO299784).

[2] The author's work is supported in part by the Department of Energy (DE-FG02-04ER25620).

[3] The author's work is supported in part by the Department of Energy (DE-FG02-04ER25620), the National Science Foundation (DMS-0107832), and the Sandia Corporation (PO299784).

0168-874X/$ - see front matter © 2008 Elsevier B.V. All rights reserved.
doi:10.1016/j.finel.2008.10.011

are difficult to correct. In the case of the conjugate heat transfer, the operator decomposition causes a loss in the order of the numerical approximation.

In this paper, we perform an *a posteriori* error analysis of a finite element implementation of the operator decomposition technique and obtain accurate error estimates that are used to guide an adaptive postprocessing strategy. Our approach is based on the standard techniques using variational analysis, residuals, and the generalized Green's function solution to an adjoint problem [1–6], which we modify to account for several new features arising from the operator decomposition.

The operator decomposition approach taken in this paper is different from the operator splitting approaches considered in, e.g. [7–9]. Traditionally, operator splitting approaches modify the solution operator in such a way that the stability properties are changed. This is recognized in [7] as a difference between the adjoint of the global system and the adjoint of the individual components, which must be accounted for in the error analysis. In this paper, we use the operator decomposition to iteratively construct the fully implicit solution to the global system within each time step. The advantage of this approach is that this allows the use of the global adjoint problem to compute the *a posteriori* error estimate. The feasibility of this approach relies on the iterative method converging quickly, which is addressed in [10].

In addition to obtaining accurate estimates, we seek to improve the accuracy of the operator decomposition method in an efficient way. In particular, we adapt the "boundary flux recovery" technique developed by Wheeler [11] and Carey [12,13] to compute normal derivatives on a boundary, and show that this can be used to improve accuracy, and in particular, restore the order of convergence of the numerical approximation that is lost due to the transfer of error in the operator decomposition.

In Section 2, we introduce the conjugate heat transfer problem and provide some notation. In Section 3, we describe the iterative operator decomposition finite element method and some modifications, as well as the boundary flux recovery method used to compute gradients on the common interface. We perform an *a posteriori* error analysis in Section 4, using the adjoint to the global problem. In Section 5, we use our error analysis to identify the transferred gradient information as being responsible for the loss of order of the numerical approximation and show that using the recovered boundary flux restores the order of convergence. In Section 6, we numerically approximate the solution to the adjoint problem corresponding to a quantity of interest and use the error indicator to determine when the postprocessed flux needs to be computed. Our conclusions are presented in Section 7.

2. The model for conjugate heat transfer

Let Ω_1 and Ω_2 be polygonal domains in $\mathbb{R}^2$ or $\mathbb{R}^3$ with boundaries $\partial\Omega_1$ and $\partial\Omega_2$ intersecting along an interface $\Gamma = \partial\Omega_1 \cap \partial\Omega_2$. We consider a system of parabolic equations, where the components are coupled through boundary conditions imposed on Γ,

$$\begin{cases} \dfrac{\partial u_1}{\partial t} + L_1 u_1 = f_1, & (\boldsymbol{x}, t) \in \Omega_1 \times (0, t_N], \\ u_1 = u_{1,0}, & (\boldsymbol{x}, t) \in \Omega_1 \times \{0\}, \\ u_1 = 0, & (\boldsymbol{x}, t) \in \partial\Omega_1 \backslash \Gamma \times (0, t_N], \\ \begin{cases} u_1 = u_2, \\ A_1 \partial_n u_1 = A_2 \partial_n u_2, \end{cases} & (\boldsymbol{x}, t) \in \Gamma \times (0, t_N], \\ \dfrac{\partial u_2}{\partial t} + L_2 u_2 = f_2, & (\boldsymbol{x}, t) \in \Omega_2 \times (0, t_N], \\ u_2 = u_{2,0}, & (\boldsymbol{x}, t) \in \Omega_2 \times \{0\}, \\ u_2 = 0, & (\boldsymbol{x}, t) \in \partial\Omega_2 \backslash \Gamma \times (0, t_N], \end{cases} \tag{2.1}$$

where $i = 1, 2$, $L_i u_i = -\nabla \cdot (A_i \nabla u_i) + c_i u_i$, $A_i \geqslant A_{i,0} > 0$, c_i, f_i are sufficiently smooth functions, and ∂_n is the partial derivative in the direction of the unit normal vector that is directed outwards from $\partial\Omega_1$. We assume the initial values satisfy the boundary conditions and the interface condition. The results of this paper extend easily to general linear parabolic operators and general Dirichlet, Neumann, and Robin boundary conditions on the boundaries in the complement of the interface.

We let $L^2(\Omega_i)$ denote the space of square integrable functions on Ω_i with inner product $(\cdot,\cdot)_{\Omega_i}$ and norm $\|\cdot\|_{\Omega_i}$, but use $(\cdot,\cdot) = (\cdot,\cdot)_{\Omega_i}$ when the domain is clear. We use $H^s(\Omega_i)$ to denote the Sobolev space with real index s associated with the norm $\|\cdot\|_{\Omega_i,s}$ and seminorm $|\cdot|_{\Omega_i,s}$. We also use the subspaces $H_0^1(\Omega_i) = \{v \in H^1(\Omega_i), v = 0 \text{ on } \partial\Omega_i \backslash \Gamma\}$.

3. An iterative operator decomposition method

We consider iterative operator decomposition methods to compute the numerical solution to (2.1). We define the iterative procedure within each time step, and in this paper we only consider splittings where each component uses the same time scale. Applications of operator splitting to multi-scale problems can be found in [7,9].

3.1. Finite element discretization

Our error analysis is based on a variational formulation and adjoint operators, so we use a discontinuous Galerkin method to discretize in time [4,7,14–16] combined with a continuous Galerkin method in space [17,18].

We first discretize $(0, T]$ into $0 = t_0 < t_1 < \cdots < t_N = T$ with time steps $\{\Delta t_n\}_{n=1}^N$, $\Delta t_n = t_n - t_{n-1}$, $I_n = (t_{n-1}, t_n]$, and $\Delta t = \max_{1 \leqslant n \leqslant N} (\Delta t_n)$. Let W_n^r denote the space of polynomials of degree r on I_n, and let ρ denote a projection onto W_n^r. Note that we are allowing functions to be discontinuous across time nodes and we denote the jump across t_n by $[w]_n = w_n^+ - w_n^-$ where $w_n^\pm = \lim_{s \to t_n \pm} w(s)$.

We let $T_{i,h}$ be a triangulation of Ω_i into elements K where the length of the longest edge is h_K and $h_i = \max_{K \in T_{i,h}} h_K$. We assume that each triangulation is locally quasi-uniform and $\overline{\Omega}_i = \bigcup_{K \in T_{i,h}} K$. However, the triangulations on either side of Γ are not assumed to be aligned.

We use the piecewise polynomial spaces

$$V_1^q = \{v \text{ continuous on } \Omega_1,\ v \in P^q(K) \text{ for all } K \in T_{1,h}\}$$

$$V_2^q = \{v \text{ continuous on } \Omega_2,\ v \in P^q(K) \text{ for all } K \in T_{2,h}\}$$

and the associated spaces

$$V_{1,0}^q = \{v \in V_1^q | v = 0, \boldsymbol{x} \in \partial\Omega_1\},$$

$$V_{2,0}^q = \{v \in V_2^q | v = 0, \boldsymbol{x} \in \partial\Omega_2 \backslash \Gamma\},$$

where $P^q(K)$ denotes the space of polynomials of degree q on an element K. Note that V_1^q and V_2^q consist of continuous polynomials in space. We let π_i be a projection into V_i^q as well as the projection into V_i^q along the interface Γ.

The operator decomposition finite element method is summarized in Algorithm 1.

Algorithm 1. Operator decomposition finite element method.

for $n = 1, 2, 3, \ldots, N$ **do**
Given $U_1^{n,\{0\}} = U_1^{n-1}$ and $U_2^{n,\{0\}} = U_2^{n-1}$
for $(k = 1, 2, 3, \ldots)$ **do**
(a) Given $U_2^{n,\{k-1\}}$ on the interface, find $U_1^{n,\{k\}} \in V_1^q \times W_n^r$ such that

$$\int_{I_n} \left(\left(\frac{\partial U_1^{n,\{k\}}}{\partial t}, v_1 \right) + a_1(U_1^{n,\{k\}}, v_1) \right) \mathrm{d}t + ([U_1^{n,\{k\}}]_{n-1}, v_1(\boldsymbol{x}, t_{n-1})) = \int_{I_n} (f_1, v_1)\, \mathrm{d}t \tag{3.1}$$

for all $v_1 \in V_{1,0}^q \times W_n^r$, with,

$$\begin{cases} U_1^{n,\{k\}} = U_1^{n-1}, & (\boldsymbol{x}, t) \in \Omega_1 \times \{t_{n-1}\}, \\ U_1^{n,\{k\}} = 0, & (\boldsymbol{x}, t) \in \partial\Omega_1 \backslash \Gamma \times I_n, \\ U_1^{n,\{k\}} = \rho\pi_1 U_2^{n,\{k-1\}}, & (\boldsymbol{x}, t) \in \Gamma \times I_n. \end{cases} \tag{3.2}$$

(b) Compute a numerical flux $\theta^{n,\{k\}} \approx A_1 \partial_n u_1^n$
(c) Find $U_2^{n,\{k\}} \in V_2^q \times W_n^r$ such that

$$\int_{I_n} \left(\left(\frac{\partial U_2^{n,\{k\}}}{\partial t}, v_2 \right) + a_2(U_2^{n,\{k\}}, v_2) \right) \mathrm{d}t + ([U_2^{n,\{k\}}]_{n-1}, v_2(\boldsymbol{x}, t_{n-1})) = \int_{I_n} ((f_2, v_2) + (\theta^{n,\{k\}}, v_2)_\Gamma)\, \mathrm{d}t \tag{3.3}$$

for all $v_2 \in V_{2,0}^q \times W_n^r$, with,

$$\begin{cases} U_2^{n,\{k\}} = U_2^{n-1}, & (\boldsymbol{x}, t) \in \Omega_2 \times \{t_{n-1}\}, \\ U_2^{n,\{k\}} = 0, & (\boldsymbol{x}, t) \in \partial\Omega_2 \backslash \Gamma \times I_n. \end{cases} \tag{3.4}$$

(d) Check convergence criteria.
(e) If converged, set $U_1^n = U_1^{n,\{k\}}$ and $U_2^n = U_2^{n,\{k\}}$.
end for
end for

Here, n denotes the time step and $\{k\}$ denotes the iteration at step n. Throughout this paper, we iterate until $\int_{I_n} \|U_1^{n,\{k\}} - \rho\pi_1 U_2^{n,\{k\}}\|_\Gamma \, \mathrm{d}t$ is less than a prescribed tolerance, i.e., until the continuity condition in the fully coupled problem is satisfied to within a given tolerance.

3.2. Numerical quadrature

Typically, the integrals in (3.1) and (3.3) are computed using numerical quadrature. In the case $r = 0$ and the single quadrature point $t_n \in I_n$, Eqs. (3.1) and (3.3) simplify to

$$a_1^n(U_1^{n,\{k\}}, v_1(\boldsymbol{x}, t_n)) + \frac{1}{\Delta t_n}([U_1^{n,\{k\}}]_{n-1}, v_1(\boldsymbol{x}, t_{n-1})) = (f_1^n, v_1(\boldsymbol{x}, t_n))$$

and

$$a_2^n(U_2^{n,\{k\}}, v_2(\boldsymbol{x}, t_n)) + \frac{1}{\Delta t_n}([U_2^{n,\{k\}}]_{n-1}, v_2(\boldsymbol{x}, t_{n-1})) = (f_2^n, v_2(\boldsymbol{x}, t_n)) + (\theta^{n,\{k\}}, v_2(\boldsymbol{x}, t_n))_\Gamma$$

respectively, which is closely related to the backward Euler difference scheme [4,19]. We have used the obvious notation for the evaluation of the bilinear forms and data at t_n.

The remainder of this paper analyzes the error in the case $q = 1$ and $r = 0$, i.e., the continuous piecewise linear finite element method in space and the discontinuous piecewise constant finite element method in time with right-endpoint quadrature, although similar results are conjectured to hold in the general case.

3.3. Iterative convergence

The overall computational cost of the operator decomposition finite element method is greatly influenced by the number of iterations required in each time step. Unfortunately, the simple iterative scheme in Algorithm 1 may converge slowly, and may even diverge for certain values of A_1 and A_2 along the interface [20,21], certain geometries [22–24], or large time steps [25].

Recently, innovative algorithms have been developed to accelerate the convergence of the operator decomposition finite element method. For example, consider the following relaxation scheme. We choose $\alpha \in [0, 1)$ and update the Dirichlet interface values with

$$U_1^{n,\{k\}} = \alpha U_1^{n,\{k-1\}} + (1 - \alpha)\rho\pi_1 U_2^{n,\{k-1\}}. \tag{3.5}$$

Optimal values of α can be found in [23,24] for elliptic problems with $A_1 = A_2$, but optimal relaxation parameters are often difficult to find for the general problem.

This difficulty prompted the development of Newton–Krylov methods [10,26] which, given a sufficiently accurate initial guess, are guaranteed to solve the fixed point problem in a finite, and usually small, number of iterations. We do not pursue this issue further, but rather we derive an error representation which does not depend on the choice of iterative acceleration and focus on analyzing the loss in accuracy.

3.4. Flux correction

In Section 5, we show that operator decomposition results in a loss of order of convergence of the finite element solution with respect to the spatial mesh size h_1. This is not completely unexpected due to the lower order of accuracy in the derivative, which reduces the order of the overall approximation. To mitigate this effect, we extend the postprocessing technique developed by Wheeler [11] and Carey [12,13] to compute a more accurate boundary flux for a time dependent problem.

We define the set of elements in $T_{1,h}$ that intersect the boundary by

$$T_{1,h}^\Gamma = \{K \in T_{1,h} | \overline{K} \cap \Gamma \neq \emptyset\}$$

and the corresponding space

$$V_{1,\Gamma}^q = \{v \in P^q(K) \quad \text{with } K \in T_{1,h}^\Gamma, v(\eta_i) = 0 \text{ if } \eta_i \notin \Gamma\}, \tag{3.6}$$

where $\{\eta_i\}$ denotes the nodes of element K, so the degrees of freedom correspond to the nodes on the boundary. This space will arise later as the difference between a projection onto $T_{1,h}$ and a second projection onto $T_{1,h}$ that is also required to be zero on the boundary. We seek $\sigma^{n,\{k\}} \in V_{1,\Gamma}^q \times W_n^r$ satisfying

$$\int_{I_n} (\sigma^{n,\{k\}}, v)_\Gamma \, \mathrm{d}t = ([U_1^{n,\{k\}}]_{n-1}, v(\boldsymbol{x}, t_{n-1})) + \int_{I_n} \left(\left(\frac{\partial U_1^{n,\{k\}}}{\partial t}, v \right) + a_1(U_1^{n,\{k\}}, v) - (f_1, v) \right) \mathrm{d}t \tag{3.7}$$

for all $v \in V^q_{1,\Gamma} \times W^r_n$, where $U_1^{n,\{k\}}$ is the iterative approximation. Green's identity implies that $\sigma^{n,\{k\}}$ gives an approximation to the normal flux on the boundary which is relatively inexpensive to compute.

In general, the accuracy of the recovered boundary flux approximation depends on the regularity of an associated Green's function [20,27,28]. In some cases, though perhaps not all, the postprocessed flux has the same accuracy as the finite element approximation. However, we show that the recovered boundary flux leads to a cancelation of the "transfer error" term in the error representation formula, which is the source of the loss of order. This fortunate cancelation of errors means the accuracy of this recovered boundary flux is only of peripheral interest for our purposes.

4. *A posteriori* error analysis

To estimate the error of the operator decomposition finite element approximation, we apply *a posteriori* techniques based on variational analysis and the adjoint problem.

In the discussion below, we assume k_n iterations are computed on I_n and we use $\theta^{n,\{k_n\}}$ to denote the numerical flux passed from Ω_1 to Ω_2 over I_n. Let

$$e_i^n = u_i(\boldsymbol{x}, t_n) - U_i^{n,\{k_n\}}$$

denote the error at time t_n.

The adjoint boundary value problem for the quantity of interest $(\boldsymbol{\psi}, \boldsymbol{e}^N) = (\psi_1, e_1^N) + (\psi_2, e_2^N)$ for the coupled problem (2.1) is

$$\begin{cases} -\dfrac{\partial \phi_1}{\partial t} + L_1^* \phi_1 = 0, & (\boldsymbol{x}, t) \in \Omega_1 \times (t_N, 0], \\ \phi_1 = \psi_1, & (\boldsymbol{x}, t) \in \Omega_1 \times \{t_N\}, \\ \phi_1 = 0, & (\boldsymbol{x}, t) \in \partial\Omega_1 \backslash \Gamma \times (t_N, 0], \\ \begin{cases} \phi_1 = \phi_2, \\ A_1 \partial_n \phi_1 = A_2 \partial_n \phi_2, \end{cases} & (\boldsymbol{x}, t) \in \Gamma \times (t_N, 0], \\ -\dfrac{\partial \phi_2}{\partial t} + L_2^* \phi_2 = 0, & (\boldsymbol{x}, t) \in \Omega_2 \times (t_N, 0], \\ \phi_2 = \psi_2, & (\boldsymbol{x}, t) \in \Omega_2 \times \{t_N\}, \\ \phi_2 = 0, & (\boldsymbol{x}, t) \in \partial\Omega_2 \backslash \Gamma \times (t_N, 0], \end{cases} \tag{4.1}$$

where $L_i^* \phi_i = -\nabla \cdot (A_i \nabla \phi_i) + c_i \phi_i$. We solve (4.1) numerically by using an iterative operator decomposition algorithm, Algorithm 1. The number of iterations and the numerical flux can be chosen independently of the forward problem. We use the notation $\phi_i^n = \phi_i(\boldsymbol{x}, t_n)$ as before.

An error representation formula is derived using the standard procedure described in, e.g., [1,4,20]. We multiply the adjoint system by the error, integrate by parts in time, apply the divergence theorem in space, and apply Galerkin orthogonality. In the case of the operator decomposition finite element method, we must be careful with the terms along the interface. Terms that typically drop out in the error analysis, remain due to the fact that the solution is not continuous across the interface. In addition, the test space $V^q_{1,0}$ consists of functions which are zero along the interface, while, in general, the adjoint solution is not. Thus, additional terms involving the space $V^q_{1,\Gamma}$ arise and must be handled accordingly. The details of this procedure can be found in [20,25] for coupled elliptic problems, and in [21,25] for a coupled nonlinear system.

Theorem 4.1. *The errors* $e_1^N = u_1(\boldsymbol{x}, t_N) - U_1^{n,\{k_n\}}$ *and* $e_2^N = u_2(\boldsymbol{x}, t_N) - U_2^{n,\{k_n\}}$ *for the operator decomposition finite element method with* $q = 1$ *and* $r = 0$ *satisfy,*

$$\|e_1^N\|_{\Omega_1} + \|e_2^N\|_{\Omega_2} = E_1 + E_2 + E_3 + E_4 + E_5 + E_6 + E_7,$$

where

$$E_1 = (\phi_1^0, (I - \pi_1) u_{1,0}) + (\phi_2^0, (I - \pi_2) u_{2,0}) \tag{4.2}$$

represents the initial error due to projecting the initial condition onto the spatial discretization,

$$E_2 = \sum_{n=1}^N \int_{I_n} \left\{ \left((I - \pi_1)\phi_1^{n-1}, \frac{1}{\Delta t_n} [U_1^{n,\{k_n\}}]_{n-1} \right) + (f_1, (I - \pi_1)\phi_1) - a_1(U_1^{n,\{k_n\}}, (I - \pi_1)\phi_1) \right\} \mathrm{d}t \tag{4.3}$$

represents the spatial discretization errors over $\Omega_1 \times (0, t_N]$,

$$E_3 = \sum_{n=1}^N \int_{I_n} \left\{ \left((I - \pi_2)\phi_2^{n-1}, \frac{1}{\Delta t_n} [U_2^{n,\{k_n\}}]_{n-1} \right) + (f_2, (I - \pi_2)\phi_2) - a_2(U_2^{n,\{k_n\}}, (I - \pi_2)\phi_2) \right\} \mathrm{d}t \tag{4.4}$$

represents the spatial discretization errors over $\Omega_2 \times (0, t_N]$,

$$E_4 = \sum_{n=1}^N \int_{I_n} \left\{ \left((I - \rho)\pi_1\phi_1^{n-1}, \frac{1}{\Delta t_n} [U_1^{n,\{k_n\}}]_{n-1} \right) + (f_1, (I - \rho)\pi_1\phi_1) - a_1(U_1^{n,\{k_n\}}, (I - \rho)\pi_1\phi_1) \right\} \mathrm{d}t \tag{4.5}$$

represents the time discretization errors over $\Omega_1 \times (0, t_N]$,

$$E_5 = \sum_{n=1}^N \int_{I_n} \left\{ \left((I - \rho)\pi_2\phi_2^{n-1}, \frac{1}{\Delta t_n} [U_1^{n,\{k_n\}}]_{n-1} \right) + (f_2, (I - \rho)\pi_2\phi_2) - a_2(U_2^{n,\{k_n\}}, (I - \rho)\pi_2\phi_2) \right\} \mathrm{d}t \tag{4.6}$$

represents the time discretization errors over $\Omega_2 \times (0, t_N]$,

$$E_6 = \sum_{n=1}^N \int_{I_n} \{ (A_1 \partial_n \phi_1, U_1^{n,\{k_n\}} - U_2^{n,\{k_n\}})_\Gamma \} \mathrm{d}t \tag{4.7}$$

represents the iteration error in terms of the jump across the interface, and finally,

$$E_7 = \sum_{n=1}^N \int_{I_n} \{ (\theta^{n,\{k_n\}}, \rho\pi_2\phi_2) - (\sigma^{n,\{k_n\}}, \rho\pi_1\phi_1) \} \mathrm{d}t, \tag{4.8}$$

represents the transfer error due to passing the numerical flux.

The choice of derivative information transferred from Ω_1 to Ω_2 has a significant impact on the transfer component.

- Suppose we set $\theta^{n,\{k_n\}} = A_1 \partial_n U_1^{n,\{k_n\}}$, then

$$E_7 = \sum_{n=1}^N \int_{I_n} ((A_1 \partial_n U_1^{n,\{k\}} - \sigma^{n,\{k\}}, \rho\pi_2\phi_2)_\Gamma + (\sigma^{n,\{k\}}, \rho\pi_2\phi_2 - \rho\pi_1\phi_1)_\Gamma) \mathrm{d}t, \tag{4.9}$$

  which represents a transfer error and a projection error.
- Suppose we set $\theta^{n,\{k\}} = \sigma^{n,\{k\}}$, then

$$E_7 = \sum_{n=1}^N \int_{I_n} (\sigma^{n,\{k\}}, \rho\pi_2\phi_2 - \rho\pi_1\phi_1)_\Gamma \mathrm{d}t,$$

  which represents only a projection error with *no transfer error.*

5. An analysis of the loss of order

In practice, the iterative operator decomposition algorithm defined in Algorithm 1 with $q=1$ and $r=0$ is occasionally observed to result in $\mathbf{O}(h_1+\Delta t)$ convergence rather than the $\mathbf{O}(h_1^2+\Delta t)$ convergence that is obtained when solving the fully coupled problem. This loss of order occurs when passing the normal derivative of the finite element approximation, which is only $\mathbf{O}(h_1+\Delta t)$. Passing the recovered boundary flux restores the full order of convergence. We use the adjoint problem and the error representation in Theorem 4.1 to derive *a posteriori* error bounds for the iterative approximations. Numerical examples are provided at the end of the section.

5.1. L^2 error bounds

Let u_1 and u_2 be sufficiently smooth solutions to (2.1), and $U_1^{n,\{k_n\}}$ and $U_2^{n,\{k_n\}}$ be the solutions to the operator decomposition scheme at t_n after k_n iterations. Let $\theta^{n,\{k_n\}}$ denote the flux passed at the k_n^{th} iteration. Let ϕ_1 and ϕ_2 solve the adjoint problem (4.1) with $\psi_1=e_1^N/\|e_1^N\|_{\Omega_1}$ and $\psi_2=e_2^N/\|e_2^N\|_{\Omega_2}$.

We construct Lemmas 5.1–5.7 to bound E_1–E_7 individually. In each of these lemmas we first provide the general bound when the triangulations do not match across the boundary, if applicable, and then show the simplification that arises for matching triangulations. We present Lemmas 5.1–5.7 without proof and direct the reader to [4,18] for a detailed analysis in the case of matching triangulations [25,28] and in the case of nonmatching triangulations. The proofs of Lemmas 5.6 and 5.7 are similar to results in [20,21,25]. We then combine these seven lemmas into Theorems 5.8 and 5.10 which give error bounds for the operator decomposition finite element method when $\theta^{n,\{k\}}=A_1\partial_n U_1^{n,\{k\}}$, and when $\theta^{n,\{k\}}=\sigma^{n,\{k\}}$, respectively. These two theorems describe the general result when the triangulations do not match across the boundary while the simplification given matching triangulations is provided as a corollary.

Lemma 5.1 (*Bound on* E_1).

$$E_1\leqslant Ch_1^2S_{11}R_{11}+Ch_2^2S_{12}R_{12},$$

where S_{11} *and* S_{12} *are stability factors depending only on* $\phi_1^0=\phi_1(\boldsymbol{x},0)$ *and* $\phi_2^0=\phi_2(\boldsymbol{x},0)$, *respectively, and* R_{11} *and* R_{12} *depend on* $u_{1,0}$ *and* $u_{2,0}$, *respectively.*

Lemma 5.2 (*Bound on* E_2). *If the triangulations* $T_{1,h}$ *and* $T_{2,h}$ *do not match along the interface, then*

$$E_2\leqslant\sum_{n=1}^{N}C(h_1^2S_{21}^nR_{21}^n+h_1^{3/2}S_{22}^nR_{22}^n)$$

and if the triangulations match along the interface, then

$$E_2\leqslant\sum_{n=1}^{N}C(h_1^2S_{21}^nR_{21}^n),$$

where S_{21}^n *and* S_{22}^n *are stability factor depending only on* ϕ_1 *and* $\pi_1\phi_1$, *respectively, and* R_{21}^n *and* R_{22}^n *are residuals depending on* $(1/\Delta t_n)[U_1^{n,\{k_n\}}]_{n-1}$, f_1, $U_1^{n,\{k_n\}}$, *and* $U_2^{n,\{k_n-1\}}$.

Lemma 5.3 (*Bound on* E_3). *If the triangulations* $T_{1,h}$ *and* $T_{2,h}$ *do not match along the interface, then*

$$E_3\leqslant\sum_{n=1}^{N}C(h_2^2S_{31}^nR_{31}^n+h_2^{3/2}S_{32}^nR_{32}^n)$$

and if the triangulations match along the interface, then

$$E_3\leqslant\sum_{n=1}^{N}C(h_2^2S_{31}^nR_{31}^n),$$

where S_{31}^n *and* S_{32}^n *are stability factors depending only on* ϕ_2 *and* $\pi_2\phi_2$,, *respectively, and* R_{31}^n *and* R_{32}^n *are residuals depending on* $(1/\Delta t_n)[U_2^{n,\{k_n\}}]_{n-1}$, f_2, $U_2^{n,\{k_n\}}$, *and* $U_1^{n,\{k_n\}}$.

Lemma 5.4 (*Bound on* E_4).

$$E_4\leqslant\sum_{n=1}^{N}C(\Delta t_nS_{41}^nR_{41}^n),$$

where S_{41}^n *is a stability factor depending only on* $\pi_1\phi_1$ *and* R_{41}^n *is a residual depending on* $(1/\Delta t_n)[U_1^{n,\{k_n\}}]_{n-1}$, f_1, $U_1^{n,\{k_n\}}$, *and* $U_2^{n,\{k_n-1\}}$.

Lemma 5.5 (*Bound on* E_5).

$$E_5\leqslant\sum_{n=1}^{N}C(\Delta t_nS_{51}^nR_{51}^n),$$

where S_{51}^n *is a stability factor depending only on* $\pi_2\phi_2$ *and* R_{51}^n *is a residual depending on* $(1/\Delta t_n)[U_2^{n,\{k_n\}}]_{n-1}$, f_2, $U_2^{n,\{k_n\}}$, *and* $U_1^{n,\{k_n\}}$.

Lemma 5.6 (*Bound on* E_6). *If the triangulations* $T_{1,h}$ *and* $T_{2,h}$ *do not match along the interface, then*

$$E_6\leqslant\sum_{n=1}^{N}C(S_{61}^n\|U_1^{n,\{k_n\}}-\pi_1U_2^{n,\{k_n\}}\|_\Gamma+h_1^{3/2}S_{62}^nR_{62}^n+h_2^{3/2}S_{63}^nR_{63}^n)$$

and if the triangulations match along the interface, then

$$E_6\leqslant\sum_{n=1}^{N}CS_{61}^n\|U_1^{n,\{k_n\}}-\pi_1U_2^{n,\{k_n\}}\|_\Gamma$$

where S_{61}^n *and* S_{62}^n *are stability factors depending only on* ϕ_1 *and* ϕ_2, *respectively, and* R_{61}^n *is a residual depending on* f_1, $U_1^{n,\{k_n\}}$, *and* $U_2^{n,\{k_n-1\}}$, *and* R_{62}^n *is a residual depending on* f_2, $U_1^{n,\{k_n\}}$, *and* $U_2^{n,\{k_n\}}$.

Lemma 5.7 (*Bound on* E_7).

(i) *If the triangulations* $T_{1,h}$ *and* $T_{2,h}$ *do not match along the interface and* $\theta^{n,\{k_n\}}=A_1\partial_nU_1^{n,\{k_n\}}$, *then*

$$E_7\leqslant\sum_{n=1}^{N}C(h_1^{\beta_1}S_{71}^nR_{71}^n+h_1^{\beta_2}S_{72}^nR_{72}^n+h_1^{3/2}S_{73}^nR_{73}^n+h_2^{3/2}S_{74}^nR_{74}^n)$$

(ii) *If the triangulations* $T_{1,h}$ *and* $T_{2,h}$ *match along the interface and* $\theta^{n,\{k_n\}}=A_1\partial_nU_1^{n,\{k_n\}}$, *then*

$$E_7\leqslant\sum_{n=1}^{N}C(h_1^{\beta_1}S_{71}^nR_{71}^n+h_1^{\beta_2}S_{72}^nR_{72}^n).$$

(iii) *If the triangulations* $T_{1,h}$ *and* $T_{2,h}$ *do not match along the interface and* $\theta^{n,\{k_n\}}=\sigma^{n,\{k_n\}}$, *then*

$$E_7\leqslant\sum_{n=1}^{N}C(h_1^{3/2}S_{73}^nR_{73}^n+h_2^{3/2}S_{74}^nR_{74}^n).$$

(iv) *If the triangulations $T_{1,h}$ and $T_{2,h}$ match along the interface and $\theta^{n,\{k_n\}} = \sigma^{n,\{k_n\}}$, then*

$$E_7 = 0,$$

where S_{71}^n and S_{72}^n are stability factors depending only on ϕ_1 and ϕ_2, respectively, R_{71}^n is a residual depending on f_1, $U_1^{n,\{k_n\}}$, and $U_2^{n,\{k_n-1\}}$, and R_{72}^n is a residual depending on f_2, $U_1^{n,\{k_n\}}$, and $U_2^{n,\{k_n\}}$.

Remark 5.1. In practice, the error in the normal derivative is typically the same accuracy as the H^1 error, namely $\mathbf{O}(h_1 + \Delta t)$. However, an application of the trace theorem only proves $\mathbf{O}(h_1^{1/2} + \Delta t)$ accuracy. This is not an important issue, however, since we intend to use the fact that this term is less accurate than the others, and therefore pollutes the L^2 error. We assume the error in the normal derivative converges $\mathbf{O}(h_1^{\beta_1} + \Delta t)$ for $1/2 \leqslant \beta_1 \leqslant 1$, and the recovered flux converges $\mathbf{O}(h_1^{\beta_2} + \Delta t)$ $\beta_1 \leqslant \beta_2 \leqslant 2$ [27,28]. In certain situations, the recovered boundary flux is the same order as the finite element approximation [11–13], but this result is not known in general. We emphasize that the accuracy of the recovered boundary flux is immaterial due to the cancelation in the error representation.

The bounds in Lemmas 5.1–5.7 are combined in the following theorems and corollaries. First we consider the case $\theta^{n,\{k\}} = A_1 \partial_n U_1^{n,\{k\}}$.

Theorem 5.8. *Assume the triangulations $T_{1,h}$ and $T_{2,h}$ do not match along the interface Γ, and $\theta^{n,\{k_n\}} = A_1 \partial_n U_1^{n,\{k_n\}}$. Then the errors $e_1^N = u_1 - U_1^{N,\{k_N\}}$ and $e_2 = u_2 - U_2^{N,\{k_N\}}$ satisfy*

$$\begin{aligned}\|e_1^N\|_{\Omega_1} + \|e_2^N\|_{\Omega_2} \leqslant\ & Ch_1^2 S_{11} R_{11} + Ch_2^2 S_{12} R_{12} \\ & + \sum_{n=1}^{N} \{Ch_1^2 (S_{21}^n R_{21}^n) + Ch_2^2 (S_{31}^n R_{31}^n) \\ & + C\Delta t_n (S_{41}^n R_{41}^n + S_{51}^n R_{51}^n) \\ & + Ch_1^{3/2} (S_{22}^n R_{22}^n + S_{62}^n R_{62}^n + S_{73}^n R_{73}^n) \\ & + Ch_2^{3/2} (S_{32}^n R_{32}^n + S_{63}^n R_{63}^n + S_{74}^n R_{74}^n) \\ & + CS_{61}^n \|U_1^{n,\{k_n\}} - \rho\pi_1 U_2^{n,\{k_n\}}\|_\Gamma \\ & + Ch_1^{\beta_1} S_{71}^n R_{71}^n + Ch_1^{\beta_2} S_{72}^n R_{72}^n\}\end{aligned}$$

with $1/2 \leqslant \beta_1 \leqslant 1$, $\beta_1 \leqslant \beta_2 \leqslant 2$, and stability factors and residuals defined in Lemmas 5.1–5.7.

Corollary 5.9. *Assume the triangulations $T_{1,h}$ and $T_{2,h}$ match along the interface Γ, and $\theta^{n,\{k_n\}} = A_1 \partial_n U_1^{n,\{k_n\}}$. Then the errors $e_1^N = u_1 - U_1^{N,\{k_N\}}$ and $e_2 = u_2 - U_2^{N,\{k_N\}}$ satisfy*

$$\begin{aligned}\|e_1^N\|_{\Omega_1} + \|e_2^N\|_{\Omega_2} \leqslant\ & Ch_1^2 S_{11} R_{11} + Ch_2^2 S_{12} R_{12} \\ & + \sum_{n=1}^{N} \{Ch_1^2 (S_{21}^n R_{21}^n) + Ch_2^2 (S_{31}^n R_{31}^n) \\ & + C\Delta t_n (S_{41}^n R_{41}^n + S_{51}^n R_{51}^n) \\ & \nu + CS_{61}^n \|U_1^{n,\{k_n\}} - \rho\pi_1 U_2^{n,\{k_n\}}\|_\Gamma \\ & + Ch_1^{\beta_1} S_{71}^n R_{71}^n + Ch_1^{\beta_2} S_{72}^n R_{72}^n\}\end{aligned}$$

with $1/2 \leqslant \beta_1 \leqslant 1$, $\beta_1 \leqslant \beta_2 \leqslant 2$, and stability factors and residuals defined in Lemmas 5.1–5.7.

Theorem 5.8 and Corollary 5.9 is valid independently of the size of $\|U_1^{\{k\}} - \rho\pi_1 U_2^{\{k\}}\|_\Gamma$, but when the iteration converges such that this term is negligible, it is clear that the term containing $h_1^{\beta_1}$ decreases at a slower rate than the other terms. Suppose that we set $\theta^{n,\{k_n\}} = \sigma^{n,\{k_n\}}$ instead of the finite element flux. As shown in Lemma 5.7, this reduces E_7 to

$$E_7 = \sum_{n=1}^{N} (\sigma^{n,\{k_n\}}, \rho\pi_2\phi_2 - \rho\pi_1\phi_1)_\Gamma$$

resulting in the following theorem.

Theorem 5.10. *Assume the triangulations $T_{1,h}$ and $T_{2,h}$ do not match along the interface Γ, and $\theta^{n,\{k_n\}} = \sigma^{n,\{k_n\}}$. Then the errors $e_1^N = u_1 - U_1^{N,\{k_N\}}$ and $e_2 = u_2 - U_2^{N,\{k_N\}}$ satisfy*

$$\begin{aligned}\|e_1^N\|_{\Omega_1} + \|e_2^N\|_{\Omega_2} \leqslant\ & Ch_1^2 S_{11} R_{11} + Ch_2^2 S_{12} R_{12} \\ & + \sum_{n=1}^{N} \{Ch_1^2 (S_{21}^n R_{21}^n) + Ch_2^2 (S_{31}^n R_{31}^n) \\ & + C\Delta t_n (S_{41}^n R_{41}^n + S_{51}^n R_{51}^n) \\ & + Ch_1^{3/2} (S_{22}^n R_{22}^n + S_{62}^n R_{62}^n + S_{73}^n R_{73}^n) \\ & + Ch_2^{3/2} (S_{32}^n R_{32}^n + S_{63}^n R_{63}^n + S_{74}^n R_{74}^n) \\ & + CS_{61}^n \|U_1^{n,\{k_n\}} - \rho\pi_1 U_2^{n,\{k_n\}}\|_\Gamma\}\end{aligned}$$

with stability factors and residuals defined in Lemmas 5.1–5.7.

Corollary 5.11. *Assume the triangulations $T_{1,h}$ and $T_{2,h}$ match along the interface Γ, and $\theta^{n,\{k_n\}} = \sigma^{n,\{k_n\}}$. Then the errors $e_1^N = u_1 - U_1^{N,\{k_N\}}$ and $e_2 = u_2 - U_2^{N,\{k_N\}}$ satisfy*

$$\begin{aligned}\|e_1^N\|_{\Omega_1} + \|e_2^N\|_{\Omega_2} \leqslant\ & Ch_1^2 S_{11} R_{11} + Ch_2^2 S_{12} R_{12} \\ & + \sum_{n=1}^{N} \{Ch_1^2 (S_{21}^n R_{21}^n) + Ch_2^2 (S_{31}^n R_{31}^n) \\ & + C\Delta t_n (S_{41}^n R_{41}^n + S_{51}^n R_{51}^n) \\ & + CS_{61}^n \|U_1^{n,\{k_n\}} - \rho\pi_1 U_2^{n,\{k_n\}}\|_\Gamma\}\end{aligned}$$

with stability factors and residuals defined in Lemmas 5.1–5.7.

Comparing Theorem 5.10 with Theorem 5.8 and Corollary 5.11 with Corollary 5.9, we see that the terms involving h^{β_1} and h^{β_2} have dropped out and the optimal order of convergence of the numerical approximation has been restored.

5.2. Numerical results

Example 5.1. Let $\Omega_1 = [0,1] \times [0,1]$ and $\Omega_2 = [1,2] \times [0,1]$ and assume that the triangulations match along $\Gamma = \{(x,y) | x = 1, 0 \leqslant y \leqslant 1\}$.

Table 1
Comparison of the convergence rates for the operator decomposition finite element method in Example 5.1 when passing the finite element flux, $A_1\partial_n U_1^{n,\{k\}}$, and when passing the recovered boundary flux, $\sigma^{n,\{k\}}$

$h_1 = h_2$	FEM flux	Conv. rate	Boundary flux	Conv. rate
1/8	2.524e−1		7.988e−2	
1/16	1.342e−1	0.91	2.044e−2	1.97
1/32	6.693e−2	1.00	5.133e−3	1.99
1/64	3.319e−2	1.01	1.289e−3	1.99

Consider the coupled heat equations:

$$\begin{cases} \dfrac{\partial u_1}{\partial t} - \Delta u_1 = f_1, & (\boldsymbol{x},t) \in \Omega_1 \times (0,t_N], \\ u_1 = 0, & (\boldsymbol{x},t) \in \Omega_1 \times \{0\}, \\ u_1 = 0, & (\boldsymbol{x},t) \in \partial\Omega_1 \backslash \Gamma \times (0,t_N], \\ \begin{cases} u_1 = u_2, \\ \partial_n u_1 = \partial_n u_2, \end{cases} & (\boldsymbol{x},t) \in \Gamma \times (0,t_N], \\ \dfrac{\partial u_2}{\partial t} - \Delta u_2 = f_2, & (\boldsymbol{x},t) \in \Omega_2 \times (0,t_N], \\ u_2 = 0, & (\boldsymbol{x},t) \in \Omega_2 \times \{0\}, \\ u_2 = 0, & (\boldsymbol{x},t) \in \partial\Omega_2 \backslash \Gamma \times (0,t_N], \end{cases} \tag{5.1}$$

where the data $f_1(x,y)$ and $f_2(x,y)$ are chosen so the true solutions are

$$u_1 = u_2 = \sin\left(\frac{\pi}{10}t\right)\sin\left(\frac{9\pi}{2}x\right)\sin(\pi y).$$

We choose a true solution which is relatively easy to resolve in time, but difficult to resolve in space to guarantee that the space discretization error will dominate the approximation. We discretize using continuous piecewise linear finite elements in space and discontinuous piecewise constant polynomials in time, and apply Algorithm 1. We set $\Delta t = 0.1$ and iterate within each time step until $\|U_1^{n,\{k\}} - \rho\pi_1 U_2^{n,\{k\}}\|_\Gamma < 10^{-6}$. In Table 1, we compare the L^2 error at $t = 1$ when passing the finite element flux and when passing the recovered flux. The results confirm the convergence rates predicted in Corollaries 5.9 and 5.11 for matching triangulations.

6. Adaptive postprocessing

The *a posteriori* error estimate (4.2)–(4.8) can be used to adaptively refine the spatial mesh as well as the time discretization to accurately compute a quantity of interest [1,20,28]. The standard approach is to approximate the adjoint solution corresponding to the quantity of interest and use (4.2)–(4.8) to compute local error indicators over each space-time element and mark an element for refinement if the local indicator is sufficiently large.

In this paper, we are interested in estimating and correcting the transfer error that arises due to passing the finite element flux. Despite the fact that computing the recovered flux is relatively cheap, we only want to compute this postprocessed flux if it affects our quantity of interest. Therefore, we propose the "adaptive" algorithm described in Algorithm 2.

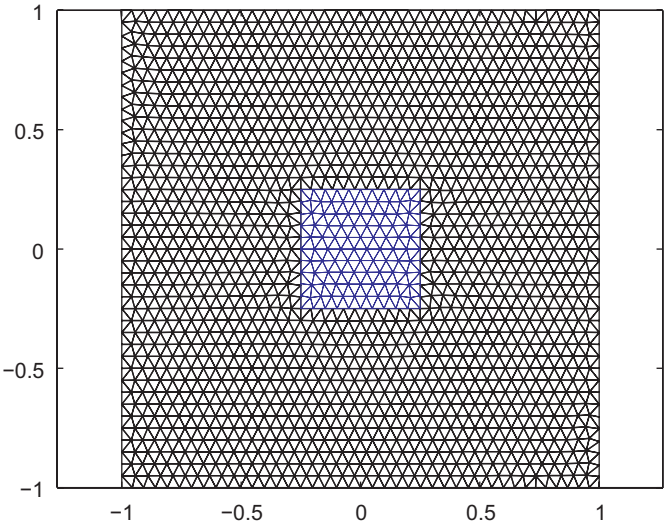

Fig. 1. Computational domains and spatial discretizations for Example 6.1.

Algorithm 2. Adaptive postprocessing algorithm.

(1) Solve the forward problem (2.1) on a given space-time discretization with

$$\theta^{n,\{k_n\}} = A_1\partial_n u_1^{n,\{k_n\}}.$$

(2) Solve the adjoint problem corresponding to a quantity of interest.
(3) Compute the error estimate using (4.2)–(4.8).
(4) If the transfer error indicator,

$$\eta_n = \left| \int_{I_n} ((\theta^{n,\{k_n\}}, \rho\pi_2\phi_2) - (\sigma^{n,\{k_n\}}, \rho\pi_1\phi_1))\,\mathrm{d}t \right|,$$

is larger than a given tolerance on a subinterval, mark the subinterval for postprocessing.
(5) Recompute the solution on the marked subintervals using the recovered flux.

Example 6.1. Let $\Omega_1 = [-0.25, 0.25] \times [-0.25, 0.25]$ and $\Omega_2 = [-1,1] \times [-1,1] \backslash \Omega_1$ triangulated as shown in Fig. 1. Note that the meshes do not match along the interface. Consider the coupled heat equations,

$$\begin{cases} \dfrac{\partial u_1}{\partial t} - \nabla \cdot (A_1 \nabla u_1) = f_1, & (\boldsymbol{x},t) \in \Omega_1 \times (0,t_N], \\ u_1 = 0, & (\boldsymbol{x},t) \in \Omega_1 \times \{0\}, \\ \begin{cases} u_1 = u_2, \\ A_1\partial_n u_1 = A_2\partial_n u_2, \end{cases} & (\boldsymbol{x},t) \in \Gamma \times (0,t_N] \\ \dfrac{\partial u_2}{\partial t} - \nabla \cdot (A_2 \nabla u_2) = f_2, & (\boldsymbol{x},t) \in \Omega_2 \times (0,t_N], \\ u_2 = 0, & (\boldsymbol{x},t) \in \Omega_2 \times \{0\}, \\ u_2 = 0, & (\boldsymbol{x},t) \in \partial\Omega_2 \backslash \Gamma \times (0,t_N], \end{cases} \tag{6.1}$$

with thermal conductivities $A_1 = 1$ and $A_2 = 100$, and forcing functions $f_1 = 0$ and $f_2 = 10\sin(3\pi t)$. We are interested in controlling a functional of the error in the inner box at $t_N = 1$ given by (e_1^N, ψ_1) where

$$\psi_1 = \frac{400}{\pi}\mathrm{e}^{-400x^2 - 400y^2},$$

which approximates a delta function at $(0,0)$.

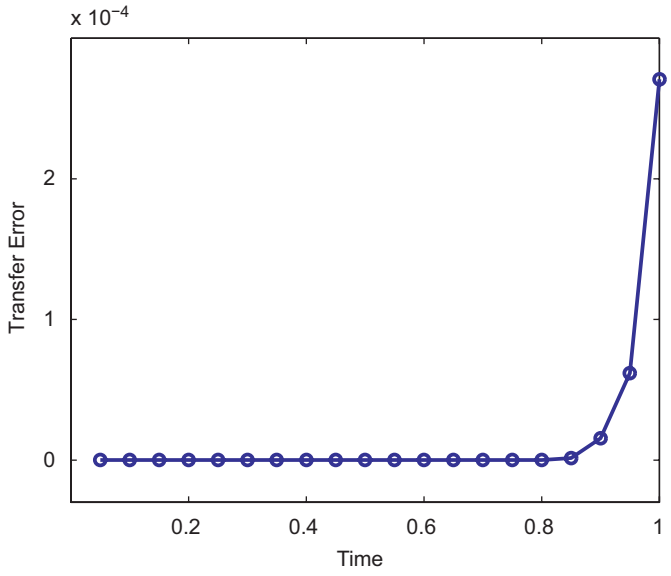

Fig. 2. Transfer error indicators for Example 6.1 when passing the finite element flux.

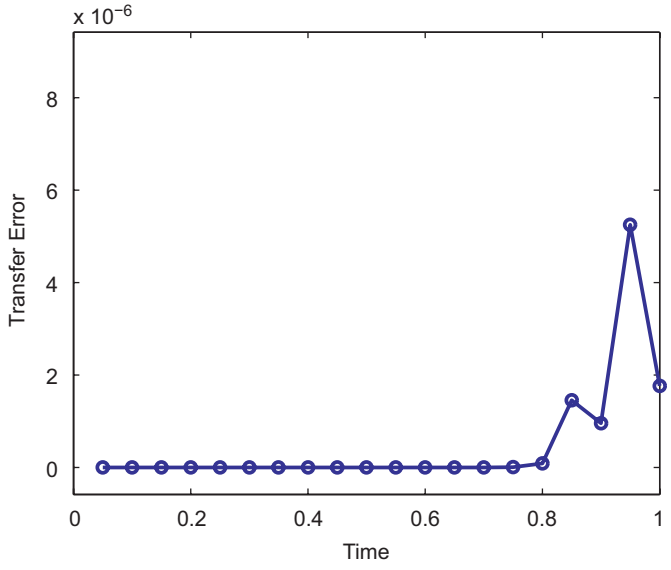

Fig. 3. Transfer error indicators for Example 6.1 when passing the recovered boundary flux.

First, we use the operator decomposition finite element method, Algorithm 1, to solve (6.1) continuous linear polynomials in space, and discontinuous constant polynomials in time with $\Delta t = 0.05$, passing the finite element flux for each iteration. Within each time step, we iterate until $\|U_1^{n,\{k\}} - \rho\pi_1 U_2^{n,\{k\}}\|_\Gamma < 10^{-6}$.

Next, we use the operator decomposition finite element method, Algorithm 1, to solve the adjoint problem (4.1) corresponding to our quantity of interest using continuous quadratic polynomials in space, and discontinuous linear polynomials in time using the same Δt. Again, we iterate until $\|\phi_1^{n,\{k\}} - \rho\pi_1\phi_2^{n,\{k\}}\|_\Gamma < 10^{-6}$.

Over each subinterval, we compute the transfer error indicator,

$$\eta_n = \left| \int_{I_n} ((\theta^{n,\{k_n\}}, \rho\pi_2\phi_2) - (\sigma^{n,\{k_n\}}, \rho\pi_1\phi_1))\,\mathrm{d}t \right|.$$

We plot these error indicators in Fig. 2. We also compute the indicators for the spatial, temporal, and iteration errors, but in this paper our interest is showing how to control the transfer error, so we do not report the other indicators.

We mark a subinterval for postprocessing if $\eta_n > 10^{-5}$. In this case, only the last three subintervals are marked. This indicates that the error in our quantity of interest has a relatively strong dependence of the transfer error in the last three time steps. The decay of this dependence is influenced by the decay of the generalized Green's function, and while the rapid decay in Fig. 2 is characteristic of strongly dissipative problems such as the heat equation, this is not necessarily the case for general parabolic operators [4,5,7].

To adaptively postprocess the flux, we go back and resolve the problem over the marked subintervals, this time passing the recovered boundary flux. In Fig. 3, we see that the transfer error has been greatly reduced in the last three subintervals. Note the difference in scale between Figs. 2 and 3. These error indicators include a projection error component owing to the fact that the meshes do not match along the interface, and thus, are not exactly zero.

7. Conclusion

We have conducted an *a posteriori* error analysis of a finite element implementation of an operator decomposition strategy for a canonical conjugate heat transfer problem. By modifying the standard approach based on variational analysis, residuals and the generalized Green's function, we derive accurate error estimates and use these estimates to guide adaptive postprocessing. Modifications to the standard error analysis account for the transfer of error between components of the decomposed operator and interpolation error. We show that the loss of order typically observed in the operator decomposition method is due to inaccuracy of the transferred gradient information and we show how the boundary flux method can be used to efficiently regain the expected optimal order of convergence.

References

[1] W. Bangerth, R. Rannacher, Adaptive Finite Element Methods for Differential Equations, Birkhauser, Basel, 2003.
[2] T. Cao, D.W. Kelly, M. Ainsworth, Some useful techniques for pointwise and local error estimates of the quantities of interest in the finite element approximation, ANZIAM J. 42 (2000) 317–339.
[3] D. Estep, M. Holst, M. Larson, Generalized Green's functions and the effective domain of influence, SIAM J. Sci. Comput. 26 (2005) 1314–1339.
[4] D. Estep, M.G. Larson, R.D. Williams, Estimating the error of numerical solutions of systems of reaction–diffusion equations, Mem. Am. Math. Soc. 146 (696) (2000) viii+109.
[5] D. Estep, A posteriori error bounds and global error control for approximations of ordinary differential equations, SIAM J. Numer. Anal. 32 (1995) 1–48.
[6] V. Heuveline, R. Rannacher, Duality-based adaptivity in the HP-finite element method, J. Numer. Math 11 (2003) 95–113.
[7] D. Estep, V. Ginting, D. Ropp, J. Shadid, S. Tavener, A posteriori a priori analysis of multiscale operator splitting, SIAM J. Numer. Anal. 46 (2008) 1116–1146.
[8] D.L. Ropp, J.N. Shadid, Stability of operator splitting methods for systems with indefinite operators: reaction–diffusion systems, J. Comput. Phys. 203 (2) (2005) 449–466.
[9] C.N. Dawson, M.F. Wheeler, Time-splitting methods for advection–diffusion–reaction equations arising in contaminant transport, in: ICIAM 91, Washington, DC, 1991, SIAM, Philadelphia, PA, 1992, pp. 71–82.
[10] D. Estep, S. Tavener, T. Wildey, The variational Newton–Krylov iteration for coupled multiphysics problems, SIAM J. Sci. Comp., submitted for publication, 2008.
[11] M.F. Wheeler, A Galerkin procedure for estimating the flux for two-point boundary-value problems using continuous piecewise-polynomial spaces, Numer. Math 2 (1974) 99–109.
[12] M.K. Seager, G.F. Carey, S.S. Chow, Approximate boundary-flux calculations, Comput. Methods Appl. Mech. Eng. 50 (1985) 107–120.
[13] G.F. Carey, Derivative calculation from finite element solutions, Comput. Methods Appl. Mech. Eng. 35 (1982) 1–14.
[14] D. Estep, A.M. Stuart, The dynamical behavior of the discontinuous Galerkin method and related difference schemes, Math. Comput. 71 (239) (2002) 1075–1103.

[15] M. Delfour, W. Hager, F. Trochu, Discontinuous Galerkin methods for ordinary differential equations, Math. Comput. 36 (154) (1981) 455–473.
[16] M.C. Delfour, F. Dubeau, Discontinuous polynomial approximations in the theory of one-step, hybrid and multistep methods for nonlinear ordinary differential equations, Math. Comput. 47 (175) (1986) 169–189 (S1–S8, with a supplement).
[17] S.C. Brenner, L.R. Scott, The Mathematical Theory of Finite Element Methods, Springer, Berlin, 2002.
[18] K. Eriksson, D. Estep, P. Hansbo, C. Johnson, Computational Differential Equations, Cambridge University Press, Cambridge, 1996.
[19] D. Estep, D. French, Global error control for the continuous Galerkin finite element method for ordinary differential equations, RAIRO Modél. Math. Anal. Numér 28 (1994) 815–852.
[20] D. Estep, S. Tavener, T. Wildey, A posteriori analysis and improved accuracy for an operator decomposition solution of a conjugate heat transfer problem, SIAM J. Numer. Anal. 46 (2008) 2068–2089.
[21] D. Estep, S. Tavener, T. Wildey, A posteriori error estimation and adaptive mesh refinement for a multi-discretization operator decomposition approach to fluid–solid heat transfer, J. Comput. Phys., submitted for publication, 2008.
[22] M.B. Giles, Stability analysis of numerical interface boundary conditions in fluid-structure thermal analysis, Int. J. Numer. Methods Fluids 25 (1997) 421–436.
[23] J.R. Rice, P. Tsompanopoulus, E. Vavalis, Interface relaxation methods for elliptic differential equations, Appl. Numer. Math. 32 (2000) 219–245.
[24] D. Yang, A parallel nonoverlapping Schwarz domain decomposition method for elliptic interface problems, IMA J. Numer. Anal. 16 (1996) 75–91.
[25] T. Wildey, A posteriori analysis of operator decomposition on interface problems, Ph.D. Thesis, Colorado State University, 2007.
[26] I. Yotov, Interface solvers and preconditioners of domain decomposition type for multiphase flow in multiblock porous media. Adv. Comput.: Theory and Practice 7 (2001) 157–167.
[27] M. Giles, M.G. Larson, J.M. Levenstam, E. Suli, Adaptive error control for finite element approximations of the lift and drag coefficients in viscous flow, Technical Report NA-97-06, Oxford University Computing Laboratory, 1997.
[28] T. Wildey, D. Estep, S. Tavener, A posteriori error estimation of boundary flux, Commun. Numer. Methods Eng. 24 (2008) 421–434.